ELSEVIER

Solar Energy Materials & Solar Cells 72 (2002) 231–246

Solar Energy Materials & Solar Cells

www.elsevier.com/locate/solmat

Defect passivation of industrial multicrystalline solar cells based on PECVD silicon nitride

F. Duerinckx*, J. Szlufcik

IMEC, Kapeldreef 75, 3001 Leuven, Belgium

Abstract

Low surface recombination velocity and significant improvements in bulk quality are key issues for efficiency improvements of solar cells based on a large variety of multicrystalline silicon materials. It has been proven that PECVD silicon nitride layers provide excellent surface and bulk passivation and their deposition processes can be executed with a high throughput as required by the PV industry. The paper discusses the various deposition techniques of PECVD silicon nitride layers and also gives results on material and device properties characterisation. Furthermore the paper focuses on the benefits achieved from the passivation properties of PECVD SiN_x layers on the multi-Si solar cells performance. This paper takes a closer look at the interaction between bulk passivation of multi-Si by PECVD SiN_x and the alloying process when forming an Al-BSF layer. Experiments on state-of-the-art multicrystalline silicon solar cells have shown an enhanced passivation effect if the creation of the alloy and the sintering of a silicon nitride layer (to free hydrogen from its bonds) happen simultaneously. The enhanced passivation is very beneficial for multicrystalline silicon, especially if the defect density is high, but it poses processing problems when considering thin ($<200\,\mu m$) cells. © 2002 Elsevier Science B.V. All rights reserved.

Keywords: Solar cells; Multicrystalline silicon; Defects; Hydrogen passivation

1. Introduction

With the current stable growth of the PV shipments of around 30% the total world PV production will reach a GWp level already by the year 2005. Crystalline silicon solar cells constitute more than 85% of the world PV market with a tendency to increase the market share. To follow the production growth, cell manufacturers are

*Corresponding author. Tel.: 32-16-281923; fax: +32-16-281501.
E-mail address: filip.duerinckx@imec.be (F. Duerinckx).

0927-0248/02/$ - see front matter © 2002 Elsevier Science B.V. All rights reserved.
PII: S0927-0248(01)00170-2

forced to shift from good quality mono-Si wafers to different types of lower quality polycrystalline substrates: cast multi-Si wafers, ribbons and thin polycrystalline-Si films. All these materials are characterised by large inhomogeneities caused by grain boundaries and intra-grain defects like dislocation, twins and others. These inherent defected regions act as recombination centres of minority carriers.

Due to silicon supply problems, often a low quality feedstock is used, introducing various impurities in an uncontrolled way. Metallic impurities, oxygen and carbon behaving themselves as recombination centres, interact additionally with the crystallographic defects enhancing their recombination properties [1]. It is obvious that such imperfect multicrystalline silicon substrates are characterised by a very low lifetime of minority carriers. A wrongly designed cell processing sequence can increase impurity segregation at the defected regions and consequently increase their recombination activity. Therefore the thermal treatments must often be tuned to the properties of specific multi-Si materials. There are, however, several processing techniques which, when combined in a well thought-out solar cell processing sequence, can drastically improve the starting lifetime. Impurities like oxygen and metallic fast diffusers (Fe, Cu, Ni, Cr) can be efficiently extracted by external gettering occurring during the emitter diffusion from $POCl_3$ source [2] and/or during the aluminium silicon alloying process commonly used for BSF formation.

Defects, impurities and segregated impurities on extended defects can be passivated by hydrogen [3]. There are several techniques developed for hydrogen passivation of silicon bulk and surfaces. The best known are: annealing in forming gas ambient, H ion implantation, direct and remote plasma hydrogenation and deposition of H-containing silicon nitride layers (SiN_x:H).

2. Deposition techniques of the SiN_x: H layers

The hydrogen containing silicon nitride layers are becoming widely introduced in industrial crystalline silicon solar cell processes thanks to the unique possibility of combining in one processing step an antireflection coating deposition along with surface and bulk passivation [4,5]. Chemical, mechanical, optical and electrical properties of silicon nitride as well as the effectiveness of surface and bulk passivation strongly depend on the selected deposition technique. For solar cell application the most suitable are the deposition processes from the gas phase by means of chemical vapour deposition (CVD) using silane, ammonia and/or nitrogen as the reactant gases. The resulting silicon nitride layers are usually non-stoichiometric and contain up to 40 at% of hydrogen and are usually denoted in the literature as SiN_x:H. The three basic CVD processes are: atmospheric pressure (APCVD), low pressure (LPCVD) and plasma enhanced (PECVD). APCVD involves reaction of silane and ammonia at atmospheric pressure in the temperature range of 700–900°C. LPCVD involves the reaction of dichlorosilane and ammonia at reduced pressure ($\sim$0.1 Torr) and temperatures around 750°C. PECVD uses plasma-enhanced reaction of silane and ammonia (or optionally nitrogen) at reduced pressure ($\sim$1 Torr) and temperatures below 500°C. The PECVD method is of

particular interests for solar cell application. The main advantages of the PECVD method over APCVD and LPCVD are: low processing temperature, higher deposition rate, the possibility to tune the refractive index over a wide range and much larger concentration of hydrogen in the deposited layers. The refractive index of PECVD SiN_x layers can be varied in a range of 1.8 and 2.3 by means of the silane/ammonia ratio. A trade-off has to be found between minimisation of reflection and reduction of energy loss by absorption of short wavelength photons in the SiN_x:H layer. The main reason for the strong interests in PECVD SiN_x:H stem however not from the antireflection properties but mainly from the fact that there is overwhelmingly strong evidence for the very good surface and bulk passivation properties of the PECVD SiN_x:H layers. The appropriate implementation of PECVD SiN_x:H into a low-cost multicrystalline silicon solar process leads to comparable surface passivation and bulk passivation to respective dry oxide and prolonged hydrogenation passivation processes. Important pioneering work regarding SiN_x-passivation and its application to silicon solar cells has been conducted during the past decades by J. Hanoka and co-workers [6].

There are two basic different methods of PECVD SiN_x:H deposition: direct and remote PECVD. In direct PECVD reactors all processing gasses (silane, ammonia, and nitrogen) are directly injected between the electrodes and excited by an electromagnetic field. The silicon substrates are placed within the plasma. Depending on the generator frequency, one can distinguish a "low frequency" (10–500 kHz), a "high frequency" (13.56 MHz) or a "very high frequency" (30–100 MHz) direct plasma excitation. The excitation frequency influences the effectiveness of the surface and bulk passivation. Heavy ion bombardment present in a low frequency direct plasma produces a surface damage and therefore lower quality silicon surface passivation is achieved than in case of high or very high frequency direct plasma deposited SiN_x:H layers [7]. On the other hand it is believed that some surface damage enhances in-diffusion of hydrogen into silicon and helps in bulk passivation [3].

In the remote plasma CVD technique, the plasma excitation takes place outside the deposition chamber usually by means of microwaves, hollow cathode or arc jet. In most cases only ammonia or a nitrogen/hydrogen mixture are excited and directed onto a silicon substrate. Silane is injected downstream directly into the deposition chamber and is mainly dissociated by the atomic hydrogen from the plasma source. The main advantages of the RPECVD SiN_x:H are the much higher deposition rate and the absence of silicon surface damage. Important for the solar cell working conditions is that RPCVD and high frequency direct plasma are reported to provide UV stable and excellent surface passivation [7]. The broad overview on silicon nitride surface passivation of crystalline silicon solar cells can be found in [7]. There is however still a question about the extent of bulk passivation from RPECVD deposited SiN_x layers in comparison to Direct PECVD layers.

A great interest from the PV industry in implementation of the PECVD SiN_x:H layers in an industrial multi-Si solar cell process triggered the developments of dedicated high throughput deposition systems. There are several commercial systems being currently in the advanced development phase or already introduced on the

market. These systems are based either on direct plasma parallel plate reactor [8], microwave remote plasma [7,9] or very high throughput expanding thermal plasma [10].

In the next chapters the properties of direct plasma PECVD silicon nitride layers combined with a low cost screen printing process is described in detail and analysed.

3. Screen-printed multicrystalline cells with SiN_x-passivation

3.1. Process specifications

The previous paragraphs have introduced the different methods available for deposition of SiN_x-layers including direct PECVD, which is very well suited for application on silicon solar cells. At IMEC's solar cell pilot line extensive process optimisations have been conducted to improve the efficiency of multicrystalline silicon solar cells using the inherent passivation properties of silicon nitride. Experiments have shown that it is very advantageous to apply a heat treatment after silicon nitride deposition to free hydrogen, which is present in the layer at high concentrations, from its bonds to silicon and nitrogen. Consequently hydrogen can diffuse out of the layer into the cell and bind itself to dangling bonds in the defected multicrystalline material (passivation). A comparison of two process sequences, with and without a thermal treatment of the silicon nitride layer, is shown in Fig. 1.

The process with thermal treatment of the silicon nitride layer is referred to as a "firing-through" process since the front cell contacts (Ag) are fired though the nitride layer to make contact with the underlying emitter during this high temperature step. The duration and the temperature profile for this firing step are chosen to achieve a good contact (a high Fill Factor (FF)) between the emitter and the front contact. On state-of-the-art multicrystalline material, improvements of 1% absolute have been

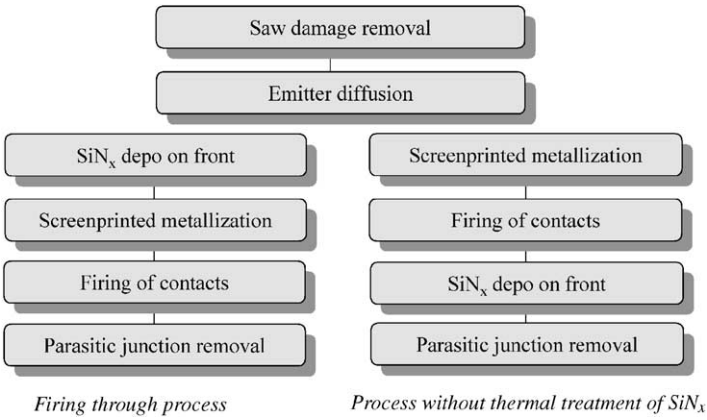

Fig. 1. Process sequence with and without thermal treatment.

obtained with the firing-through process compared to the reference process without thermal treatment of silicon nitride. Internal Quantum Efficiency measurements [11] of these cells have shown a higher response for photons of all wavelengths indicating that the improvement due to the hydrogen passivation reaches far into the bulk of the cell. For the reference process (no thermal treatment), the bulk of the cells is not affected and therefore it can be stated that no bulk passivation occurs if the nitride is not thermally treated.

The effect of the bulk passivation from the firing-through process strongly depends on the material quality. In general it can be stated that the more defected the material, the higher the improvement will be from the firing-through-SiN_x process. This is confirmed by the results of Table 1 that compare firing-through-TiO_x (no bulk passivation) and firing-through-SiN_x processes on material of lower starting quality.

This process, which is straightforward and can easily be implemented in existing production lines, can nevertheless effectively passivate the bulk of multicrystalline cells resulting in an important efficiency improvement. Although the prime purpose of the firing through process is to incorporate a bulk passivation in the process sequence, the newly developed process also brings other advantages specifically related to the use of silicon nitride. Some of these are discussed below.

3.2. Advantages of firing-through SiN_x process

3.2.1. Emitter passivation

The silicon nitride effectively passivates the emitter of silicon solar cells. This has been experimentally verified by making a comparison of cells with and without a dry oxide beneath the silicon nitride layer. The results of both groups are similar for industrial-type emitters on condition that the silicon nitride is thermally treated. If the nitride coating is not thermally treated, damage resulting from the ion bombardment during plasma deposition degrades the surface quality resulting in a J_{0e} that is twice as high (1.3×10^{-12} A/cm^2 compared to 6.2×10^{-13} A/cm^2). With thermal treatment at temperatures above 700°C, this damage is annealed.

3.2.2. Diffusion barrier

Silicon nitride acts as a diffusion barrier during contact firing. This inherent property of nitrides is well known in the microelectronics industry. Likewise the silicon nitride used in our process acts as a diffusion barrier against unwanted impurities. As a consequence, metal spikes deep into the silicon can be avoided

Table 1
Comparison of firing-through-SiN_x and TiO_x processes on defected material

Process	Jsc (mA/cm^2)	Voc (mV)	FF (%)	Eff. (%)
Firing through TiO_x	28.0	585	76.5	12.5
Firing through SiN_x	30.6	600	76.9	14.1

reducing the risk of shunting the junction and the effective metal–silicon interface stays closer to the highly doped surface region. The consequence of this is a lower series resistance and a lower ideality factor around the maximum power point. It also means that shallow emitters with a sheet resistance around 60 Ω sq. can be contacted while maintaining a good fill factor.

3.2.3. Al-BSF formation

On the back surface of most modern screen-printed solar cells, aluminium is used to create a BSF. A thick aluminium layer (20 μm) is alloyed with silicon during the sintering process of the contacts. The resulting alloyed region at the back surface of the solar cell is around 5 μm deep with an acceptor concentration that is dependent on the firing temperature used. If high enough temperatures (> 800°C) are used, the aluminium concentration in the BSF can rise to $5 \times 10^{18}\,cm^{-3}$ while the base doping level for material with a typical resistivity of 1 Ωcm is only $1.5 \times 10^{16}\,cm^{-3}$. This high/low junction effectively repels minority carriers from the back surface. Since the front contacts have to be fired through the silicon nitride layer to make contact with the emitter, an elevated firing temperature is needed which is in the optimal range for a BSF-creation. This created the opportunity to merge these two separate processing steps in one single step.

This in situ BSF-formation using the firing through process is a complementary advantage to the effect of hydrogen bulk passivation. While materials of lower quality (low base diffusion length) will be more dependent on bulk passivation, materials of higher quality (high base diffusion length) that are less dependent on bulk passivation, will benefit more from the created back-surface field. Other effects of Al-alloying and especially its synergy with SiN_x-passivation will be further discussed in Section 4.

3.2.4. Anti-reflection coating

The silicon nitride coating used in the firing-through process has a double aim: it's not only a source of hydrogen (passivation) but also acts as an excellent anti-reflection coating or ARC. This is an important advantage in comparison with other processes that incorporate bulk passivation (e.g. based on plasma hydrogenation). In that case, a separate step is still needed to deposit an ARC.

The purpose of an ARC is to reduce the reflection of incoming light photons by favouring destructive interference of photons impinging and reflecting from the Air/SiN_x/Si interface. This effect is mainly influenced by the thickness of the layer and its refractive index. Ideally the refractive index is around 2.0 for the Air/SiN_x/Si structure and around 2.3 for the encapsulated condition (Air/glass-EVA/SiN_x/Si). Since all cells are finally put into a module, the value of 2.3 is the one that's most important. However this observation makes abstraction from another feature: light absorption. When the extinction coefficient of the deposited layer rises more light will be absorbed in the layer itself. These photons will therefore not contribute to the cell current. Characterisations based on spectro-ellipsometry have indicated that this effect becomes especially important for short-wavelength light (Fig. 2). This effect is directly influenced by the NH_3/SiH_4 ratio during deposition. If more silicon is

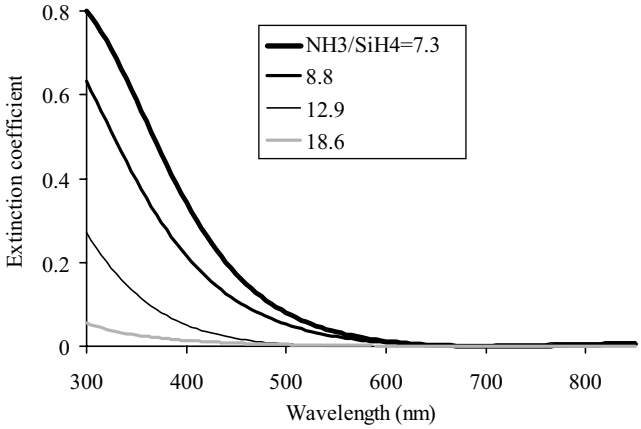

Fig. 2. Extinction coefficient of silicon nitride as a function of NH_3/SiH_4 flow ratio.

incorporated in the layer (lower NH_3/SiH_4 ratio), the extinction coefficient (and the absorption losses) as well as the refractive index will rise. At higher refractive indices, the reflection losses will be lower but this will be overcompensated by the absorption loss (higher extinction coefficient) in the layer itself. Experiments have shown that, for this reason, even for the encapsulated condition, it is favourable to limit the refractive index to values around 2.0.

3.2.5. Passivation

As was discussed earlier, a thermal treatment after the deposition of silicon nitride can release hydrogen from the Si–H and N–H bonds present in the nitride layer into the cell, passivating the silicon surface and the bulk. In our process sequence, the firing of the contacts performs this role. During the short time that the cells are at high temperature in an IR-furnace, the following actions take place simultaneously: First, the front contact is fired through the dielectric layer and makes contact with the underlying emitter. Secondly, hydrogen is released from its bonds in the nitride layer and diffuses into the cell (bulk passivation). Thirdly, the surface damage, which is a consequence of the nitride deposition in a direct PECVD-system, is annealed so that a good surface passivation is obtained. Laser beam induced current (LBIC) measurements of a typical multicrystalline cell made with the firing through silicon nitride process confirm the uniform passivation of the surface and the upper part of the bulk, independently of the grain orientation. For short wavelengths (Fig. 3(a)) the grain boundaries are invisible, passivated by the in-situ hydrogenation. The LBIC-response is displayed relative to the maximum value with a minimum value around 90%. This indicates the extent of the passivation for the upper part of the cell since most defects have been made inactive by the passivation effect. Fig. 3(b) shows the response for long wavelengths (1060 nm). These photons are absorbed uniformly throughout the cell. Therefore, the grain boundaries are more visible since the lower part of the bulk is less passivated.

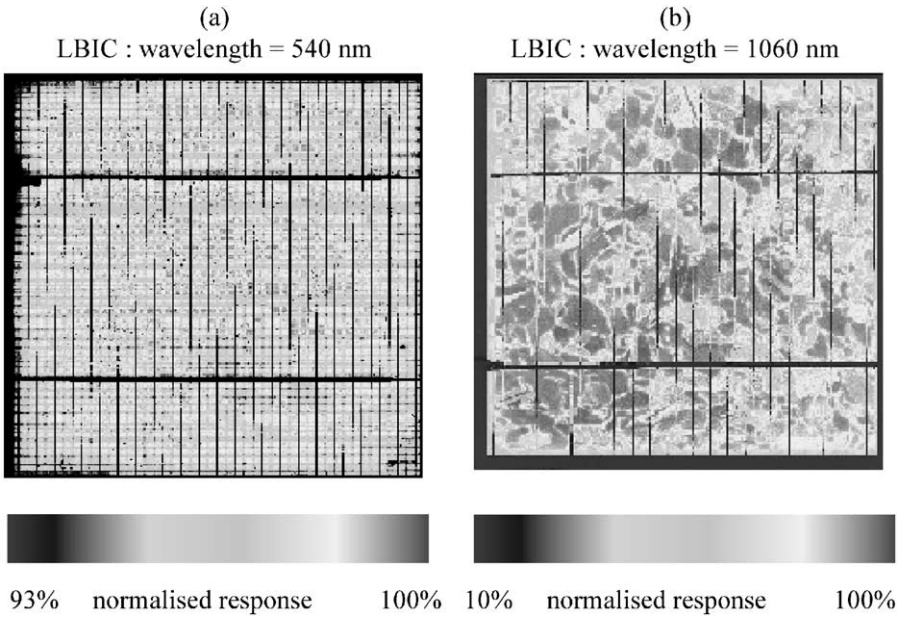

Fig. 3. LBIC measurements of cell made with a firing-through process (a) wavelength (540 nm), (b) long wavelength (1060 nm).

Table 2
Effective bulk diffusion length extracted by the spectral response analysis from 800 to 1000 nm

SiN_x present?	Firing through SiN_x?	Effective diffusion length (μm)
Yes	No	76.2
Yes	Yes	119.1

To quantify the effect of the passivation, a comparison experiment was made on neighbouring multicrystalline silicon solar cells between the firing-through process and the process without thermal treatment of the nitride layer. The cells were analysed using spectral response measurements and the effective diffusion length was extracted using Basore's method [12]. The results are shown in Table 2. It can be concluded that the effective diffusion length has increased by 56% due to the short thermal treatment of the silicon nitride (without any process complication).

3.3. Additional passivation features of SiN_x

Besides the features described above, several other issues determine the usefulness of PECVD-silicon nitride for a particular solar cell application. It is for instance well known that a high positive charge is incorporated in the first 20 nm of silicon nitride [13]. This could be confirmed by Capacitance–Voltage measurements [14] for the

Table 3
Positive fixed charge and interface-trap-density of as-deposited and sintered silicon nitride layers

Silicon nitride condition	Q_f (cm^{-2})	D_{it} (cm^2/eV)
As-deposited	3×10^{12}	2×10^{11}
Thermally treated	1×10^{12}	1×10^{11}

direct PECVD coatings deposited at IMEC's pilot line. From the CV-measurements also the interface trap density could be determined. Both parameters are given in Table 3 for as deposited and thermally treated silicon nitride layers.

It is interesting to notice that the interface trap density is reduced considerably by applying a thermal treatment. Earlier measurements confirmed the bulk passivation while these measurements indicate surface passivation. Therefore, sintering the silicon nitride layer can, at least partly, passivate damage that is a result from ion bombardment during the direct deposition process. Moreover, the positive charge is high enough to induce an inversion layer on moderately doped (around 1 Ωcm) p-type Si. Therefore silicon nitride layers should also be very suited for rear surface passivation of silicon solar cells. This could indeed be confirmed by measuring the effective surface recombination velocity (S_{eff}) of Float-zone p-silicon wafers passivated with PECVD-SiN_x. Values as low as 30 cm/s were obtained. This is an important observation for next generation solar cells.

3.4. Results of an optimised SiN_x-process on large area multicrystalline silicon solar cells

At IMEC, much effort has been put in upgrading the firing-through process and bringing it as close as possible to an industrial process ready to be implemented in production lines. While the main features of the firing-through process are similar to what was discussed in the previous paragraphs, each process step has been optimised with regard to all other process steps. Some of the most important features of the final process are:

- Isotropic texturisation [15]: a new chemical isotropic texturisation technique has been developed that replaces the standard caustic saw damage removal. This one new step removes the saw damage and at the same time randomly textures the wafers to decrease the reflection of light from the front surface.
- $POCl_3$-diffusion: a shallow emitter is used with a sheet resistance around 60 c sq. The phosphorus profile has been optimised for a maximal collection of high-energy photons.
- Parasitic junction removal: A plasma etching step has been optimised to remove the parasitic junction at the edge of the cells.
- SiN_x-deposition: As described above, the silicon nitride layer has been tailored to reduce the reflection and absorption and to increase the uniformity of the deposition.

Table 4
Results of large area cells ($12.5 \times 12.5\,cm^2$) fabricated with the firing-through-SiN_x process

Material	Emitter	ARC	Jsc (mA/cm^2)	Voc (mV)	FF (%)	Eff. (%)
Polix	Homogeneous	SiN_x	33.5	621	78.1	16.3
Eurosil	Homogeneous	SiN_x	33.5	614	77.9	16.0
Baysix	Selective	$SiN_x + MgF_2$	35.1	621	77.0	16.8
Eurosil	Selective	$SiN_x + MgF_2$	34.9	623	77.0	16.7
Polix	Selective	$SiN_x + MgF_2$	35.3	635	76.0	17.0

- Screen-printed metallisation: This step is the most critical one. The composition of the front side paste (Ag), the printing conditions (width, height and number of the fingers, width of the busbars, the printing speed, pressure and snap-off distance) and the firing conditions (temperature profile and speed) all have to be optimised in order to achieve a low series resistance in the lines as well as a low contact resistance with the emitter. This optimisation has been done taking into account the properties of the SiN_x layer (the front contact has to be fired through this layer) and the underlying emitter.

With this process, efficiencies between 15.3% and 15.7% have been achieved on large wafer batches (50–100 wafers, size: $12.5 \times 12.5\,cm^2$, resistivity: 0.5–1 Ωcm) from several different manufacturers. The series resistance of the busbar limits the efficiency of the cells. By tabbing the busbars, as is done for encapsulation of the cells into a module, the Fill Factor of the cells rises strongly and efficiencies above 16% are obtained (Table 4). These are among the highest ever measured for large cells fabricated with a straightforward process scheme.

Experiments to increase the cell efficiency further have focussed on implementing a selective emitter structure. In this more complicated process, different emitters are foreseen for the contact area (deep emitter with a high P-concentration to achieve a good contact) and for the active area (shallow emitter for a high collection of carriers created by short wavelength photons). Results of these cells with a double anti-reflection coating are also shown in Table 4.

4. Synergy between Aluminium and SiN_x

4.1. Screen-printed Al-BSF as back surface passivation

Screen printed aluminium has found a widespread use for silicon solar cells, not only in laboratory but also in production lines. It is the easiest way to create an effective BSF without unnecessarily complicating the process sequence. The Al-layer is normally printed over the whole back surface except for two strips of Ag/Al for soldering purposes. The printed layers are subsequently dried and fired. In our "firing-through" process this happens together with the front contact firing (co-firing). During this firing at high temperature, the aluminium melts and forms an

alloy with silicon according to their binary phase diagram [16]. This typically results in a 5 μm deep, highly doped p+ layer with an acceptor concentration around $5 \times 10^{18}\,cm^{-3}$. The effective surface recombination velocity as experienced by the base minority carriers is considerably reduced due to the strong electric field present at this high/low (p/p+) junction. Values below 1000 cm/s are normally obtained. Because of the simplicity and the effectiveness of the process, Al-BSF became a standard process years ago for the back surface passivation of screen-printed silicon solar cells. When PECVD-SiN_x was introduced in solar cell processes, the screen-printed aluminium back contact was already an established technology. It is more recently that researchers became aware of the dependence for a good bulk passivation on the presence of both features simultaneously, silicon nitride as well as aluminium [17,18]. This is discussed in the next paragraph.

4.2. The Al/SiN_x synergetic effect

To investigate the possible interaction between silicon nitride passivation and aluminium, the following experiment was carried out: multicrystalline Baysix wafers (size $10 \times 10\,cm^2$) were processed into solar cells according to different process sequences (Table 5). All cells were identically saw damage etched followed by a $POCl_3$-emitter diffusion. The rest of the process differed for the four groups that were made:

- Group 1: Standard process involving the co-firing of the PECVD-silicon nitride layer, the front contacts (through the silicon nitride) and the Al-layer. In this process, the creation of the BSF and the release of hydrogen from the nitride layer happen simultaneously.
- Group 2: No BSF is created. The nitride is fired together with the front (Ag) and back contacts (Ag/Al grid: only a very small amount of Al is present in this paste in order to have a good contact with p-Si).
- Group 3: The Al is fired first resulting in a BSF. The eutectic layer is removed by hot HCl, followed by deposition of SiN_x, the printing of front (Ag) and back (Ag/Al grid) contacts and firing. The resulting cell structure is exactly the same as for

Table 5
I–V results of different sequences involving SiN_x passivation and Al-BSF

Group	Process sequence	Jsc (mA/cm^2)	Voc (mV)
1	SiN_x (front)—Ag (front)—full Al (back)—firing	31.1	614
2	SiN_x (front)—Ag (front)—Ag/Al grid (back)—firing	29.8	604
3	Al (back)—firing—Al removal—SiN_x (front)—Ag (front)—Ag/Al grid (back)—firing	29.9	605
4	Al (back)—firing—Al removal—Ag (front)—Ag/Al grid (back)—firing—SiN_x (front)	27.8	589

the first group. The only difference is that the firing of the nitride and the creation of the Al-BSF do not happen simultaneously.

- Group 4: Similar to group 3, only the nitride is deposited on top of the front contacts (no annealing of the nitride layer).

Group 1 of the experiment is processed according to the standard screen printing process. In order to check the importance of Al as back contact, the second group was made using an Ag/Al grid instead of a full Al coverage. At first sight, a straightforward explanation for the rather large difference in cell results between the two groups (Table 5) would be the influence of the BSF, which is present for group 1 but not for group 2. However, this explanation was doubtful since the diffusion length is smaller than the wafer thickness of 330 μm. Therefore the BSF should not have a very large effect. To test this assumption the third group was processed: In this case, the BSF was made first followed by removal of the Al-eutectic layer, deposition of the nitride layer, screen printed metallisation of the contacts (Ag/Al grid for the back) and firing. The same results were obtained as for group 2 (no BSF) which indicates indeed that the BSF has no influence on the final cell results. It seems that the creation of the BSF together with the annealing of the nitride has a strong beneficial effect. This is seen in the IQE-curves of Fig. 4 as an improvement in the long wavelength region and indicates an extended hydrogenation effect (since the BSF does not play a role) deep into the bulk of the cell.

Group 4 shows however that, if the nitride layer is not fired at all, the results are still a lot lower. This indicates that the passivation effect from firing the nitride layer is also present when no Si–Al alloy is simultaneously created on the back surface (group 2). The effect can however be enhanced by the simultaneous creation of an alloy as can be seen from group 1. It has been proposed [18] that this enhanced effect is due to the creation of vacancies during the alloying process, which can facilitate the in-diffusion of hydrogen into the bulk.

If the enhanced passivation effect is due to the creation of vacancies during the alloying then the effect should scale with the thickness of the p+ layer that is

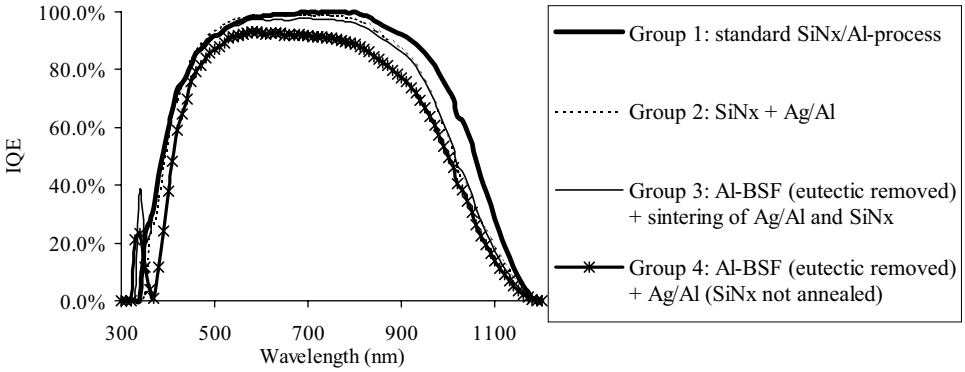

Fig. 4. IQE measurements of different sequences involving SiN_x passivation and Al-BSF.

Table 6
I–V results of cells with back contact paste (full coverage) with different Al-concentrations

Back side paste	Jsc (mA/cm^2)	Voc (mV)	FF (%)	Eff. (%)	L (μm)	S_{eff} (cm/s)
Al	32.1	618	76.8	15.2	261	1000
75% Al, 25% AgAl	31.6	614	76.4	14.8	224	1315
50% Al, 50% AgAl	31.4	612	76.5	14.7	172	2297
25% Al, 75% AgAl	30.5	606	76.1	14.1	115	34,000
AgAl	30.3	603	74.2	13.6	(107)	—

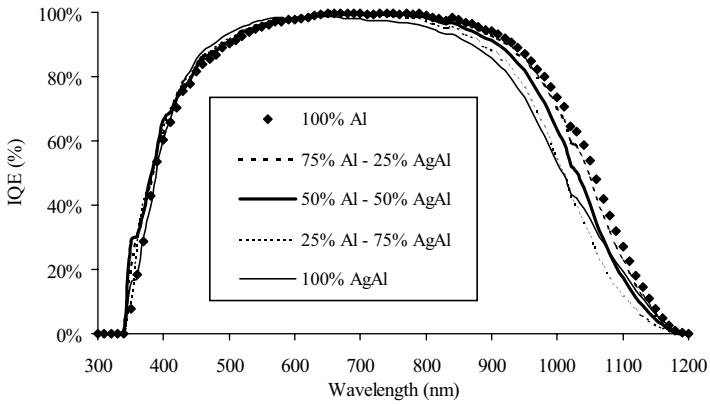

Fig. 5. IQE measurements of cells with back contact paste with different Al concentrations.

formed. To test this supposition, multicrystalline cells were made using a back contact paste with different Al-concentrations. All cells were fired at the same conditions so that the p+layer thickness (and the amount of vacancies) created in the process is only dependent on the amount of Al deposited on the wafer. The remainder of the process is identical for all wafers (saw damage removal, shallow $POCl_3$-diffusion, plasma etching, SiN_x deposition, front and backside metallisation, firing). The size of the cells was again 100 cm^2, their starting thickness was 270 μm. The results of these cells are shown in Table 6. Fig. 5 compares the IQE of the different cells. Finally, Table 6 also compares the extracted values for the base diffusion length (L) and the effective back surface recombination velocity (S_{eff}) using Basore's method [12].

The extracted values for the surface recombination velocity clearly show the effect of the BSF as expected for these thinner cells. More interesting however is the evolution of the diffusion length in the base, which also clearly scales with the Al amount in the paste. This supports the hypothesis of an enhanced diffusion of hydrogen at high temperature if simultaneously an Al-alloy is created. Note the high IQE (Fig. 5) for the cells with pure AgAl paste in the long wavelength region. This is believed to be due to a higher internal back surface reflection for this type of contact.

4.3. Short discussion

The previous experiments indeed suggest that alloying Al with Si not only result in a BSF but also improves the bulk passivation of multicrystalline cells by enhancing the in-diffusion of hydrogen. The vacancies that are created during the alloying process are very important for the creation of atomic hydrogen from molecular hydrogen [19] that can be released by cross-linking ($Si–H + N–H \rightarrow Si\text{-}N + H_2$) from the silicon nitride layer [20]. Furthermore a vacancy–hydrogen complex $\{V - H_x\}$ diffuses faster through the silicon wafer. This might explain the slightly higher IQE around wavelengths of 500 nm for the cells with a pure Ag/Al contact. In the last case a lot of hydrogen is available close to the front surface while this hydrogen can be distributed more uniformly over the wafer when a lot of vacancies are present. In the latter case this results in a higher IQE for the long wavelengths but a slightly lower one for the short wavelengths.

The results from this work clearly indicate that, in order to benefit from the enhanced passivation effect, the creation of the alloy and the release of hydrogen from silicon nitride have to happen simultaneously. If they happen sequentially, no enhanced passivation is noticed. This could mean that the created vacancies during the alloying process are lost after cooling-down and are not available afterwards.

5. Consequences and future objectives for thin cells

One of the most interesting research directions for crystalline silicon solar cells is the move towards thinner cells. The production cost savings that can be made when using thin cells drive this evolution. It is well known that the cost of the silicon material itself is a very large part of the final module cost figure. The cost of silicon crystallisation and the subsequent wafering into multicrystalline substrates has been estimated to amount to 55% of that of the finished module [21]. Therefore the use of thin wafers (thickness $<200\,\mu m$) can result in substantial savings compared to state-of-the-art cells which have a thickness around $300\,\mu m$.

However a problem arises when transferring the process based on the simultaneous processing of SiN_x and Al for these thin cells: the expansion coefficients of Al ($23.9 \times 10^{-6}\,K^{-1}$) and Si ($7.6 \times 10^{-6}\,K^{-1}$) [22] are significantly different. As a result, a wafer can be severely bent after alloying a $20\,\mu m$ thick Al-layer on a $200\,\mu m$ thick cell. This makes the module manufacturing of the cells much more difficult and can result in a sharp decrease in mechanical yield that is not acceptable. Therefore an alternative method has to be developed. Originally it was thought that the Al-layer was only important for the creation of the BSF and therefore another back surface passivation method (Boron BSF, Oxide or nitride passivation for the back surface) would yield the same or even better results. However the results of the previous paragraphs clearly indicate that the simultaneous high temperature processing of the hydrogen rich PECVD-SiN_x coating and the printed Al-layer is paramount for obtaining a good bulk passivation.

In order to solve this problem several different routes can be followed:

- Removal of the full Al back contact in a hot HCl solution after firing of the SiN_x and Al-layers (the BSF is not removed). When the Al-layer is etched off, the warping of the wafer is also removed. However, this process is complicated and environmentally unfriendly and also necessitates a second firing of the nitride layer, the front contact and the back contact (for instance a Ag/Al grid).
- Finding another method or material to obtain the same effect as with the SiN_x/Al co-firing (e.g. a material that has a better suited expansion coefficient to silicon but also alloys in a similar manner). Another possibility is the deposition of an amorphous silicon layer on the back surface with a wide bandgap (ideal for back surface passivation). This layer could also be a source of vacancies.
- Optimisation of an Al-back contact pattern that diminishes the stress level and bending problem.
- For very thin cells ($\sim 100\,\mu m$) the firing of silicon nitride on the front surface (without the presence of Al on the back) might be sufficient for an effective bulk passivation. In this case other techniques such as PECVD-SiN_x deposition can be used for back surface passivation.

It is clear that this topic is becoming one of the most important research tasks at the level of cell processing since the lower costs that are associated with thinner cells can only be benefited from if the cell efficiency can be maintained (or preferably increased). The ideal processing method for the back surface of thin cells should have the following features:

- Excellent back surface passivation (comparable or better than a state-of-the-art Al-BSF).
- Suitable for thin cells from the point of handling (high mechanical yield).
- High internal back surface reflection to reduce the loss of long wavelength photons.
- If possible, enhance the in-diffusion of hydrogen into the cells from the silicon nitride layer on the front.

References

[1] S. Martinuzzi, S. Pizzini, in: Advanced Silicon and Semiconducting Silicon Alloy Based Materials and Devices, J. Nÿs, ed., Institute of Physics Publication, Bristol, 1995, p. 323.
[2] A. Cuevas, D. Macdonald, M. Kerr, C. Samunsdett, A. Sloan, S. Shea, A. Leo, M. Macarica, S. Winderbaum, 27th IEEE Photovoltaic Specialists Conference, Anchorage, 2000, pp. 244–247.
[3] B.L. Sopori, X. Deng, J.P. Benner, A. Rohatgi, P. Sana, S.K. Estreicher, Y.K. Park, M.A. Robertson, Sol. Energy Mater. Sol. Cells 41/42 (1996) 159.
[4] K. Kimura, Tech Digest First International Photovoltaic Science and Engineering Conference, Kobe, 1984, p. 37.
[5] J. Szlufcik, K. De Clercq, P. De Schepper, J. Poortmans, A. Buczkowski, J. Nijs, R. Mertens, Proceedings of the 12th European Photovoltaic Solar Energy Conference Amsterdam, 1994, pp. 1018–1021.
[6] D.S. Ruby, W.L. Wilbanks, C.B. Fledderman, J.I. Hanoka, 13th European Photovoltaic Solar Energy Conference, Nice, 1995, pp. 1412–1414.

[7] A.G. Aberle, Sol. Energy Mater. Sol. Cells 65 (2001) 239.
[8] F. Schitthelm, P. Volk, H. Dekkers, J. Szlufcik, 16th European Photovoltaic Solar Energy Conference, Glasgow, 2000, pp. 1609–1612.
[9] W.J. Soppe, B.G. Duijvelaar, S.E.A. Schiermeier, A.W. Weber, A. Steiner, F.M. Shuurmans, 16th European Photovoltaic Solar Energy Conference, Glasgow, 2000, pp. 1420–1423.
[10] W.M.M. Kessels, Ph.D. Thesis, Eindhoven University of Technology, 2000.
[11] F. Duerinckx, J. Szlufcik, A. Ziebakowski, J. Nijs, R. Mertens, 14th European Photovoltaic Solar Energy Conference, Barcelona, 1997, p. 792.
[12] P.A. Basore, 23rd IEEE Photovoltaic Specialists Conference, Louisville, 1993, p 147.
[13] A.G. Aberle, Crystalline Silicon Solar Cells: Advanced Surface Passivation and Analysis, 1999, pp. 106.
[14] B. Bitnar, R. Glatthaar, S. Keller, J. Kugler, M. Spiegel, P. Fath, G. Willeke, E. Bucher, F. Duerinckx, J. Szlufcik, J. Nijs, R. Mertens, H. Nussbaumer, F. Ferrazza, 14th European Photovoltaic Solar Energy Conference, Barcelona, 1997, p. 1491.
[15] R. Einhaus, F. Duerinckx, J. Horzel, E. Van Kerschaver, J. Szlufcik, J. Nijs, R. Mertens, E. Vazsonyi, Second World Conference and Exhibition on Photovoltaic Solar Energy Conversion, Vienna, 1998, p. 1630.
[16] M. Hansen, K. Anderko, Constitution of Binary Alloys, 2nd Edition, McGraw-Hill Book Company, New York, 1985, pp. 132–134.
[17] A.R. Chaudhuri, K.V. Ravi, International Publication Number W089/00341, 1989.
[18] A. Rohatgi, V. Yelundur, J. Jeong, A. Ebong, D. Meier, A.M. Gabor, M.D. Rosenblum, 16th European Photovoltaic Solar Energy Conference and Exhibition, Glasgow, 2000.
[19] S.K. Estreicher, J.L. Hastings, P.A. Fedders, Phys. Rev. B 57 (20) (1998) 57.
[20] F.H.P.M. Habraken, A.E.T. Kuiper, Mater. Sci. Eng. R12 (1994) 123.
[21] T.M. Bruton, G. Luthardt, K.-D. Rasch, K. Roy, I.A. Dorrity, B. Garrard, L. Teale, J. Alonso, U. Ugalde, K. De Clercq, J. Nijs, J. Szlufcik, A. Räuber, W. Wettling, A. Vallêra, 14th European Photovoltaic Solar Energy Conference, Barcelona, 1997, p. 11.
[22] Y.S. Touloukian, R.K. Kirby, R.E. Taylor, Thermal Expansion: Metallic Elements and Alloys, IFI/Plenum, New York, 1977, pp. 14–2.